

SPEC3D: A THREE-DIMENSIONAL RADIATIVE TRANSFER CODE FOR ASTROPHYSICAL AND LABORATORY APPLICATIONS

L. Ibgui¹, I. Hubeny², T. Lanz³ and C. Stehlé¹

Abstract. We have developed a generic three-dimensional radiative transfer code, SPEC3D, aimed at post-processing 3D radiation magnetohydrodynamics simulations. SPEC3D solves the monochromatic 3D radiative transfer equation. The numerical approach and the major features of the code are presented. The wide range of applications includes the modeling of a number of astrophysical objects and structures, such as accretion shocks around young stellar objects, stellar and exoplanets atmospheres, cosmological structures, but also the modeling of laboratory astrophysics experiments such as magnetohydrodynamics jets and radiative shocks.

Keywords: radiative transfer, quantitative spectroscopy, methods: numerical, laboratory astrophysics, shock waves

1 Introduction

Radiation is a major component of many astrophysical objects. First, radiation is a probe of the physical state: the medium is analyzed through the observed spectra. Second, radiation is often strong enough to have a significant contribution to the momentum and energy budget of the medium.

With the considerable progress in computing power, it is now possible to build three-dimensional numerical models that couple the contributions of fluid dynamics, radiation, and magnetic field (if strong enough). Many 3D radiation hydrodynamics or radiation magnetohydrodynamics codes have been developed over the past few years. The treatment of radiative transfer is simplified, since such models consider the moments of the specific intensity and some kind of a closing relation between them. On the other hand, an efficient code that solves the monochromatic radiative transfer equation (RTE) is required, either to provide exact closing relations for the radiation hydrodynamics, or, more importantly, in order to compute radiation for snapshots of hydrodynamic simulations, and thus to provide a tool to analyze the physical properties of a radiating object. Several three-dimensional radiative transfer codes have been developed over the last few years (see Carlsson 2009 for a review).

We present here a generic 3D radiative transfer code, SPEC3D. We assume local thermodynamic equilibrium (LTE), and consider the time-independent form of the RTE. In § 2, we describe the formal solution solver, which applies the short-characteristics method (Kunasz & Auer 1988) in a 3D Cartesian grid, and which is coupled with efficient piecewise cubic Bezier interpolations (Auer 2003). Other features of the code are summarized in § 3. We finally present a first application to the modeling of radiative shocks experiments in § 4, which is relevant to the understanding of accretion shocks in classical T Tauri Stars.

2 3D short-characteristics

2.1 Overview of the method

The short-characteristics method can be summarized as follows. We consider a grid for which the thermophysical properties (temperature, density, velocity) are known from a prior (magneto)hydrodynamics simulation. We use

¹ LERMA, Observatoire de Paris, CNRS, UMPIC, 5, place J.Janssen, 92195 Meudon Cedex, France

² Department of Astronomy, Steward Observatory, The University of Arizona, 933 N.Cherry Ave, Tucson, AZ 85721-0065, USA

³ Department of Astronomy, University of Maryland, College Park, MD 20742-2421, USA

the integral form of the formal solution of the RTE as described hereafter. For a given direction of propagation, we consider each ray that emerges from each point of the grid. There is one ray per grid point per direction. We determine the intersection of each ray with the closest face of the corresponding upwind cubic cell. The line segment joining the intersection point with the grid point is called the short-characteristic (SC). The integral form of the RTE is then solved along this short-characteristic. There is one short-characteristic per grid point per direction. Fig. 1 shows an example of a short-characteristic defined in a 3D cartesian grid. We want to determine in the observer's frame the specific intensity in point 2 for a direction defined by polar angle θ and azimuthal angle φ . Point 1 is the intersection of the considered ray with the upwind cubic cell. We call it upwind endpoint. The short-characteristic is here defined by the line segment joining point 1 and point 2.

Let us introduce the following notations. $I(\mathbf{r}, \mathbf{n}, \nu, t)$ is the specific intensity at position \mathbf{r} for a radiation propagating in direction \mathbf{n} with frequency ν , at time t . Let us note $\chi(\mathbf{r}, \mathbf{n}, \nu, t)$ the absorption coefficient, and ds the elementary path length along the direction of propagation \mathbf{n} . The optical depth from position s_1 to position s_2 may be written as

$$\tau_{12} = \tau_{s_1 \rightarrow s_2} = \int_{s_1}^{s_2} \chi(\mathbf{r}, \mathbf{n}, \nu, t) ds \quad (2.1)$$

Let us note $I_2 = I(\mathbf{r}_2, \mathbf{n}, \nu, t)$ and $I_1 = I(\mathbf{r}_1, \mathbf{n}, \nu, t)$. The integral form of the RTE may be written along the short-characteristic joining point 1 to point 2, as

$$I_2 = I_1 e^{-\tau_{12}} + \int_0^{\tau_{12}} S(\tau) e^{-(\tau_{12}-\tau)} d\tau \quad (2.2)$$

where $S(\tau)$ is the source function $S(\mathbf{r}, \mathbf{n}, \nu, t)$.

Therefore, we can infer the specific intensity at point 2 if we know the following quantities: the specific intensity in point 1, I_1 , the source function along the short-characteristic from point 1 to point 2, and the absorption coefficient along the short-characteristic (in order to deduct the optical depth between point 1 and point 2). However, by the very nature of the problem, the source function and the absorption coefficients are specified only at the grid points. Therefore, we are essentially free to define laws of variation of these quantities along the short-characteristics, typically as low-order polynomials. Moreover, the following quantities at the upwind endpoint (point 1), intensity I_1 , optical depth τ_1 , and source function S_1 , have to be interpolated from the values in the neighbor grid points. We detail in next subsection the mathematical functions that we have adopted.

2.2 Cubic Bezier interpolations

Because of the numerous required interpolations, the short-characteristics method is known to be numerically diffusive, whether linear or second order polynomial laws be employed. Therefore, an efficient interpolation law has to be adopted. Following a suggestion by Auer (2003), we adopt Bezier cubic interpolation laws with specific adjustments.

The Bezier cubic interpolant is a polynomial of degree 3, $B(x)$, which is defined between two values of a given function $f(x)$, (x_1, f_1) and (x_2, f_2) , so that it matches the values of the function at both ends, $B(x_1) = f_1$ and $B(x_2) = f_2$, and whose derivatives at both ends, $B'(x_1)$ and $B'(x_2)$ are free values to be adjusted depending on the context. Now, we introduce a constraint of monotonicity to $B(x)$, in order to ensure its positivity between the extremal points x_1 and x_2 . This results in a range of permitted values for the derivative on the left end, $B'(x_1)$, and for the derivative on the right end, $B'(x_2)$. We choose to match the derivatives at both ends with the derivatives of the function, $B'(x_1) = f'_1$ and $B'(x_2) = f'_2$, if possible, i.e., as long as the monotonicity of the interpolant $B(x)$ is guaranteed. Such a procedure suppresses the spurious extrema encountered with a parabolic interpolation law, while ensuring a much better fit to the interpolated function than a linear or a quadratic law could provide.

Going back to the short-characteristics method, the Bezier cubic interpolant is used as an approximate of the source function between the upwind endpoint 1 and point 2 (see Fig. 1). Now, if one knows the source function value at only two points, S_1 and S_2 , then the only possibility to estimate the derivatives at both ends is to assume that they are identical and that they equal the value of the slope of the line that joins S_1 and S_2 ; one can then show that Bezier interpolant reduces to linear interpolation. It is therefore necessary, in order to increase the precision of the interpolation, to define a third point along the short-characteristic defined by point 1 and point 2. This is why we define the downwind endpoint, point 3, which is the intersection of this short-characteristic with the downwind cubic cell. Therefore, it is possible to specify a Bezier cubic interpolant

between point 1 and point 2, by defining the derivative at point 1 as the slope of the line that joins point 1 and point 2. Several possibilities exist for the estimate of the derivative at point 2, using the values at points 1, 2 and 3. The same procedure is applied for the determination of the absorption coefficient along the short-characteristic. More details will be available in a forthcoming paper.

Another issue is the determination of the physical quantities at point 1 and point 3, which are generally not grid points. To this end, we define Bezier cubic interpolants on the edges of the intersected face. Note that, while the source function and the absorption coefficients are known at each point of the grid, the specific intensity is known only in the upwind cubic cells of the current grid point that is being processed. Therefore, the sweeping of the grid must follow the direction of propagation of the radiation, to ensure that the upwind specific intensities are known before we determine the new specific intensity at a given grid point. Again, more details will soon be available in a forthcoming paper.

3 SPEC3D: major features

We have developed and validated (specifically with comparisons with well-tested 1D codes) a radiative transfer code, called SPEC3D, that determines the monochromatic formal solution of the radiative transfer equation in a three-dimensional geometry. It applies the short-characteristics method with cubic Bezier interpolations, as summarized in the preceding section. We have incorporated the possibility to define periodic boundary conditions. The user can also specify pre-defined boundary conditions. We take into account the Doppler shift of the lines. Based on the determination of the monochromatic specific intensity at each point of the grid and for each direction, the code uses Gaussian quadratures to determine the resulting moments, the mean intensity $J(\nu, x, y, z)$, the flux vector in the three directions, $F_x(\nu, x, y, z)$, $F_y(\nu, x, y, z)$, $F_z(\nu, x, y, z)$, and the six components of the radiation pressure tensor P_{xx} , P_{yy} , P_{zz} , P_{xy} , P_{xz} , P_{yz} , which all depend on (ν, x, y, z) .

4 Applications of SPEC3D

SPEC3D is a generic radiative transfer code that can be applied to simulate numerous astrophysical objects and structures, e.g., accretion shocks around young stellar objects, stellar and exoplanets atmospheres, cosmological structures. It can also be used to simulate experiments relevant to astrophysics such as magnetohydrodynamics jets and radiative shocks.

We show here a simulation of an experimental radiative shock. Such studies are an important step toward a correct modeling of spectroscopic signatures of accretion shocks in classical T Tauri Stars (Stehlé et al. 2010). Fig. 2 shows the monochromatic radiative flux in the direction of propagation of the shock, z -direction, $F_z(x, y, z, \nu)$, as calculated by SPEC3D. The radiative shock is generated in a tube full of Xenon, with a rectangular section of $1 \times 1 \text{ cm}^2$, and with the following upstream conditions: fluid velocity = 60 km s^{-1} , pressure = 7 bar, temperature = 1 eV. The lateral walls have a zero albedo: the photons can freely escape from these walls. SPEC3D post processes the hydrodynamics results provided by Matthias González* and generated by the three-dimensional radiation hydrodynamics code HERACLES (González et al. 2007). The fluid is assumed to be ideal. The objective here is to show the 3D effects of the radiation. Realistic simulations with real gas effects will be shown in a forthcoming paper (L. Ibgui, M. González et al. 2011, in preparation). The absorption coefficients are derived from an opacity database, which is based on the Screened Hydrogenic Model (Eidmann 1994; Michaut et al. 2004).

Left panel of Fig. 2 represents the flux F_z along z -axis at the center of the sections perpendicular to z -axis, for a frequency ν corresponding to an energy of $h\nu = 296 \text{ eV}$: $F_z(x = 0.5 \text{ cm}, y = 0.5 \text{ cm}, z, h\nu = 296 \text{ eV})$. The red curve represents the 3D model and the blue curve represents the 1D model (for a 1D model, the flux is obviously the same one at any point of a given section perpendicular to z -axis). The position of the hydrodynamics shock is $z = 0.10 \text{ cm}$. The radiative precursor is distinctly identified in the upstream gas (González et al. 2009 show typical profiles of a 1D radiative shock). This figure clearly reveals the difference between a 1D model and a 3D model. The maximum value of the flux F_z , reached at around $z = 0.12 \text{ cm}$, is smaller when the 3D model is applied (7.3 versus $7.7 \text{ erg}^{-1} \text{ cm}^{-2} \text{ Hz}^{-1}$) and the flux's extension in z -direction is smaller when the 3D model is applied. This is due to the lateral radiative losses, which are taken into account by SPEC3D. This result underlines the fact that a radiative shock cannot be correctly understood without considering a 3D radiative transfer model. This is also naturally a critical point for the modeling of accretion columns in T Tauri stars.

*AIM, CEA/DSM/IRFU, CNRS, Université Paris Diderot, 91191 Gif-sur-Yvette, France

Right panel of Fig. 2 represents the flux F_z at a given position in the radiative precursor $z = 0.22$ cm, $F_z(x, y, z = 0.22 \text{ cm}, h\nu = 296 \text{ eV})$. A behavior of the flux, whose value decreases as one approaches the borders, due to lateral radiative losses, is another manifestation of a 3D nature of radiative shocks.

5 Conclusions

We have presented a new generic three-dimensional radiative transfer code, SPEC3D, that solves the monochromatic 3D radiative transfer equation in Cartesian coordinates. Currently, we assume local thermodynamic equilibrium (LTE), and a time-independent situation, but both these simplifications will be removed in the future development of the code. We have employed the 3D short-characteristics method, known to be faster than the long-characteristics method, combined with performant cubic Bezier interpolation techniques.

We have shown a preliminary application to the modeling of laboratory generated radiative shocks. We have demonstrated the necessity to account for the 3D radiative transfer in 3D radiative shock structures.

We intend to apply our code to a large variety of astrophysical objects and structures, such as accretion shocks around young stellar objects, stellar and exoplanet atmospheres, cosmological structures, but also for laboratory astrophysics to study magnetohydrodynamics jets and radiative shocks.

The authors are grateful to Matthias González (AIM, CEA/DSM/IRFU, CNRS, Université Paris Diderot, 91191 Gif-sur-Yvette, France) for providing the 3D hydrodynamics results of the ideal gas shock wave simulation, which were used as an input for the radiative transfer code SPEC3D. The work is supported by French ANR, under grant 08-BLAN-0263-07.

References

- Auer, L. 2003, in *Astronomical Society of the Pacific Conference Series*, Vol. 288, *Stellar Atmosphere Modeling*, ed. I. Hubeny, D. Mihalas, & K. Werner, 3
- Carlsson, M. 2009, *Mem. Soc. Astron. Italiana*, 80, 606
- Eidmann, K. 1994, *Laser and Particle Beams*, 12, 223
- González, M., Audit, E., & Huynh, P. 2007, *A&A*, 464, 429
- González, M., Audit, E., & Stehlé, C. 2009, *A&A*, 497, 27
- Kunasz, P. & Auer, L. H. 1988, *Journal of Quantitative Spectroscopy and Radiative Transfer*, 39, 67
- Michaut, C., Stehlé, C., Leygnac, S., Lanz, T., & Boireau, L. 2004, *European Physical Journal D*, 28, 381
- Stehlé, C., González, M., Kozlova, M., et al. 2010, *Laser and Particle Beams*, 28, 253

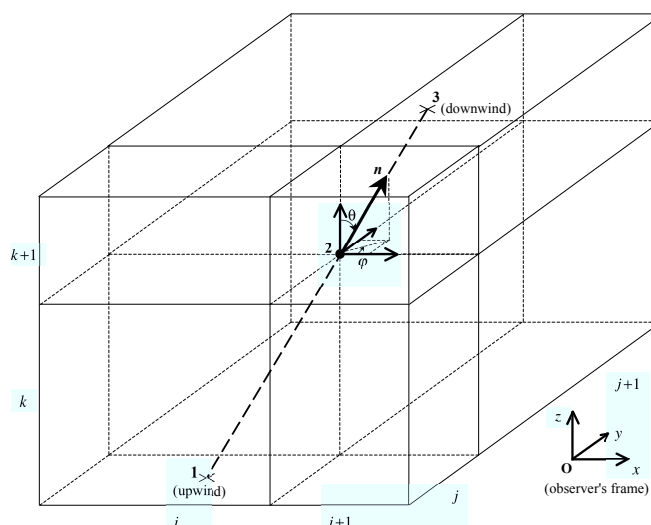


Fig. 1. The short-characteristics method illustrated with an example of a 3D cartesian grid. The specific intensity is calculated in point 2, for a radiation propagating from point 1 (upwind endpoint) to point 3 (downwind endpoint). The direction \mathbf{n} of the ray is defined by polar angle θ and azimuthal angle φ . The short-characteristic is defined by the line joining point 1 and point 2. The radiative transfer equation is solved in its integral form along this short-characteristic. The cell numbers around point 2 are $i, i+1$ in x -direction, $j, j+1$ in y -direction, and $k, k+1$ in z -direction.

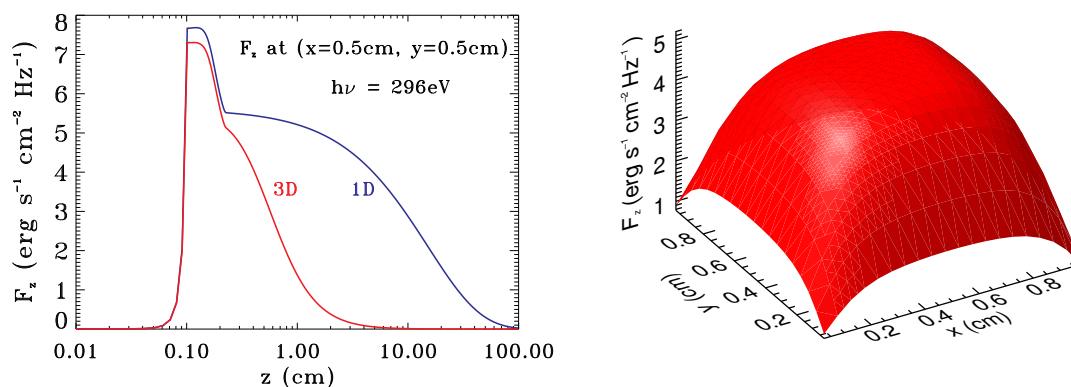


Fig. 2. Left: Monochromatic radiative flux in z -direction, $F_z(x = 0.5 \text{ cm}, y = 0.5 \text{ cm}, z, h\nu = 296 \text{ eV})$, at the center of the planes perpendicular to z -axis, emitted by a radiative shock propagating in z -direction. It is a pure Xenon flow in a cell with a rectangular section of $1 \times 1 \text{ cm}^2$. The hydrodynamics simulation makes the assumption of an ideal gas, with the following upstream conditions: fluid velocity = 60 km s^{-1} , pressure = 7 bar, temperature = 1 eV. We display the results of two hydrodynamics and radiative transfer models: the one-dimensional model is depicted by the blue curve, the three-dimensional model is represented by the red curve. See text for comments. **Right:** The same monochromatic radiative flux, but at a given z -position, $F_z(x, y, z = 0.22 \text{ cm}, h\nu = 296 \text{ eV})$. The 3D effects are clearly demonstrated by a non-constant behavior of the flux, which is due to lateral radiative losses.